na

ARTICLES

PUBLISHED ONLINE: 21 JULY 2013 | DOI: 10.1038/NPHYS2685

Mapping the orbital wavefunction of the surface states in three-dimensional topological insulators

Yue Cao[1]*, J. A. Waugh[1], X-W. Zhang[2,3], J-W. Luo[3], Q. Wang[1(], T. J. Reber[1(], S. K. Mo[4], Z. Xu[5], A. Yang[5], J. Schneeloch[5], G. D. Gu[5], M. Brahlek[6], N. Bansal[6], S. Oh[6], A. Zunger[7] and D. S. Dessau[1]*

Understanding the structure of the wavefunction is essential for depicting the surface states of a topological insulator. Owing to the inherent strong spin–orbit coupling, the conventional hand-waving picture of the Dirac surface state with a single chiral spin texture is incomplete, as this ignores the orbital components of the Dirac wavefunction and their coupling to the spin textures. Here, by combining orbital-selective angle-resolved photoemission experiments and first-principles calculations, we deconvolve the in-plane and out-of-plane *p*-orbital components of the Dirac wavefunction. The in-plane orbital wavefunction is asymmetric relative to the Dirac point. It is predominantly tangential (radial) to the *k*-space constant energy surfaces above (below) the Dirac point. This orbital texture switch occurs exactly at the Dirac point, and therefore should be intrinsic to the topological physics. Our results imply that the Dirac wavefunction has a spin–orbital texture—a superposition of orbital wavefunctions coupled with the corresponding spin textures.

The topological surface state[1–3] provides a new avenue for realizing spintronic devices and quantum computation[4,5]. Both applications require manipulating the wavefunction to achieve select spin configurations; and thus most of the research so far has focused exclusively on the spin degree of freedom[6–11]. However, because strong spin–orbit coupling is inherent in all the known topological insulators (TIs), spin is not a good quantum number and does not provide a complete description of the Dirac state. Instead, the orbital portion of the total wavefunction to which spins are strongly coupled is also critical for describing the topological surface states. It is natural to expect that the spin texture has to be locked to the orbital wavefunction in a specific manner. Actually, it is proposed that the total angular momentum **J**, defined as the sum of electron spin **s** and orbital angular momentum **L**, may be a conserved quantity[8,12]. Studying the orbital degree of freedom as well as its coupling to the helical spin texture is thus indispensable both for understanding the topological physics and for future applications.

Although the existence of the Dirac state is determined by tracking the time reversal symmetry of the bulk bands[13–15], its effective description can be constructed by considering the time reversal and real space symmetries of the surface state itself, without information from the bulk bands. To investigate which features of the Dirac state the `effective model' captures, we need to check both the spin and orbital properties of the electronic wavefunction. These questions motivate us to explore the orbital aspects of the Dirac states.

Within the prevailing description of the Dirac state[7,12,16,17], we

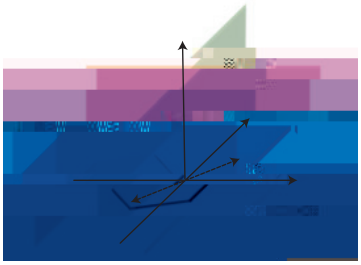

Figure 1 | ARPES energy–momentum intensity plots at the Γ point for *s* and *p* photon polarizations. a, The experimental configuration, where the sample frame is shown in red and the laboratory frame (which contains the electron detector) in blue. The sample axes can be rotated through the angle relative to the laboratory frame, though the normals of the sample and laboratory frames always stay aligned. The incident photon beam makes an angle of 7 relative to the laboratory (and sample) planes and has varying polarizations ranging from full *s* (**E** field parallel to the sample plane) to full *p* (**E** field in the orange k_x–k_z plane). **b**,**c**, ARPES cuts along the *O*–K direction of Bi_2Se_3 taken with *s* (**b**) and *p* (**c**) polarization, with the sample *O*–K axis lying in the k_x laboratory frame direction. Colour scale applies to **b**,**c**.

incident photons come at a glancing angle 7 to the sample plane and can have either *p* polarization (photon electric field vector, drawn with yellow arrow, in the orange-coloured scattering plane) or *s* polarization (**E** field perpendicular to the scattering plane). These possibilities are illustrated in Fig. 1a. In both configurations, only the electron analyser is rotated to collect data, so that the relative angles between the sample coordinate axes and the photon beam coordinates (polarization and Poynting or incident vector) remain unchanged. Detailed information about the ARPES setup and data taking can be found in Supplementary Information.

a

b

Figure 3 | Sketch of the orbital texture switch deduced from the experimental and theoretical matrix elements. a, The green orbitals are of p_z character and are viewed with p-polarized light. **b**

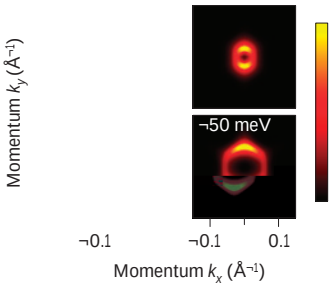

Figure 4 | OPR switches sign at the Dirac point. a,**d**, First-principles calculation of Bi_2Se_3 and Bi_2Te_3, only showing the Dirac bands (upper/lower Dirac cones in red/blue and yellow/purple solid lines for **a** and **d** respectively) and the bulk bands closest to the Dirac point. **b**, Calculated p_y orbital intensity at different energies relative to the Dirac point of Bi_2Se_3, each summed over a window of 20 meV relative to the central energy shown on the plot. **c**, For each energy relative to the Dirac point of Bi_2Se_3, the calculated projected p_y orbital intensity as a function of the sample in-plane azimuth angle (for the definition of the azimuth angle, see **b**, with 0 as marked). The dashed lines are the selected cos2 =sin2 fits to the calculated p_y intensities shown with solid lines. **e**, Calculated OPR of Bi_2Se_3 as a function of the energy relative to the Dirac point, and **f**, calculated of Bi_2Se_3 and Bi_2Te_3 as a function of momentum k. Note switches sign exactly at the Dirac point.

predicting that the in-plane tangential orbitals above the Dirac point couple with a right-handed spin texture, which is opposite to the well-known left-handed spin texture to which the out-of-plane orbitals couple. This prediction was directly confirmed by our orbital-selective and spin-resolved ARPES experiments[25], conclusively demonstrating the critical role of the orbital texture for the physics of the topological insulators.

Methods

The ARPES experiments were carried out at Beamline 10.0.1 of the Advanced Light Source, LBL. Data have been taken both from Bi_2Se_3 thin films and bulk samples and have shown consistent results. The Bi_2Se_3 thin films were prepared using a two-step growth method, as described in ref. 26 and Supplementary Information, and were protected with a Se overlayer after growth, and decapped *in situ* by heating in the final vacuum environment of the analysis chamber. The bulk samples were cleaved *in situ* at 50 K with a base pressure better than 5 10 ^{11} torr.

We carried out calculations for six quintuple-layer slabs of Bi_2Se_3 and Bi_2Te_3. The orbital character of electronic states is obtained by projecting the calculated plane-wave-based wavefunctions j $_{nk}$i onto spherical harmonics j$J_l^{R_i}Y_{lm}^{R_i}$i including p orbitals (l D 1) centred at the positions of the ions R_i.

$$\mathrm{j}\ {}_{nk}\mathrm{i}\ \mathrm{D}\ \sum_{i}^{N_a}\ \sum_{lm} {}^{R_i}_{m;nk}\mathrm{j}$$

15. Moore, J. E. & Balents, L. Topological invariants of time-reversal-invariant band structures. *Phys. Rev. B* **75,** 121306 (R) (2007).
16. Zhang, H. *et al*. Topological insulators in Bi_2Se_3, Bi_2Te_3 and Sb_2Te_3 with a single Dirac cone on the surface. *Nature Phys.* **5,** 438 442 (2009).
17. Liu, C-X. *et al*. Model Hamiltonian for topological insulators. *Phys. Rev. B* **82,** 045122 (2010).
18. Damascelli, A., Hussain, Z. & Shen, Z-X. Angle-resolved photoemission studies of the cuprate superconductors. *Rev. Mod. Phys.* **75,** 473 541 (2003).
19. Wang, Y. H. *et al*. Observation of a warped helical spin texture in Bi_2Se_3 from circular dichroism angle-resolved photoemission spectroscopy. *Phys. Rev. Lett.* **107,** 207602 (2011).
20. Ishida, Y. *et al*. Common origin of the circular-dichroism pattern in angle-resolved photoemission spectroscopy of $SrTiO_3$ and $Cu_xBi_2Se_3$. *Phys. Rev. Lett.* **107,** 077601 (2011).
21. Park, S. R. *et al*. Chiral orbital-angular momentum in the surface states of Bi_2Se_3. *Phys. Rev. Lett.* **108,** 046805 (2012).
22. Bian, G. *et al*. Illuminating the surface spin texture of the Giant-Rashba quantum-well system Bi/Ag(111) by circularly polarized photoemission. *Phys. Rev. Lett.* **108,** 186403 (2012).
23. Liang, F. Hexagonal warping effects in the surface states of the topological insulator Bi_2Te_3. *Phys. Rev. Lett.* **103,** 266801 (2009).
24. Zhang, H-J., Liu, C-X. & Zhang, S-C. Spin-orbital texture in topological insulators. Preprint at http://arxiv.org/abs/1211.0762 (2012).
25. Cao, Y. *et al*. Coupled spin-orbital texture in a prototypical topological insulator. Preprint at http://arxiv.org/abs/1211.5998 (2012).
26. Bansal, N. *et al*. Epitaxial growth of topological insulator Bi_2Se_3 film on Si(111) with atomically sharp interface. *Thin Solid Films* **520,** 224 229 (2011).
27.